

Verification of Neural Network Behaviour: Formal Guarantees for Power System Applications

Andreas Venzke, *Student Member, IEEE*, and Spyros Chatzivasileiadis, *Senior Member, IEEE*

Abstract—This paper presents for the first time, to our knowledge, a framework for verifying neural network behavior in power systems applications. Up to this moment, neural networks have been applied in power systems as a black-box; this has presented a major barrier for their adoption in practice. Developing a rigorous framework based on mixed integer linear programming, our methods can determine the range of inputs that neural networks classify as safe or unsafe, and are able to identify adversarial examples. Such methods have the potential to build the missing trust of power system operators on neural networks, and unlock a series of new applications in power systems. This paper presents the main theoretical framework and addresses concerns related to scalability and accuracy. We demonstrate our methods on the IEEE 9-bus, 14-bus, and 162-bus systems, treating both N-1 security and small-signal stability.

Index Terms—Neural networks, mixed integer linear programming, security assessment, small-signal stability.

I. INTRODUCTION

POWER system security assessment belongs to the most fundamental functions of power system operators. It is a highly computationally demanding task which considers both static security (N-1 security criterion) and dynamic security criteria (e.g. small-signal stability, transient stability, etc.). With growing uncertainty both in generation and demand, the complexity of this task further increases, calling for the development of new approaches [1].

Machine learning, such as decision trees and neural networks, has demonstrated significant potential for highly complex classification tasks including the security assessment of power systems [2]–[9]. However, the inability to anticipate the behavior of neural networks, which have been usually treated as a black box, has been posing a major barrier in the application of such methods in safety-critical systems, including power systems. This is the first work, to our knowledge, that develops provable formal guarantees that predict the behavior of neural networks for a wide range of inputs in power system applications. These methods have the potential to build the missing trust of power system operators in neural networks, and enable their application in safety-critical operations as they would no longer need to be treated as a black box.

Machine learning algorithms including neural networks have been applied in power system problems for decades. For a comprehensive review, the interested reader is referred to [2] and references therein. Recent examples include [3] which compares different machine learning techniques for probabilistic reliability assessment and shows significant reductions

in computation time compared to conventional approaches. Ref. [4] uses machine learning to predict the result of outage scheduling under uncertainty, while in [5] neural networks rank contingencies for security assessment. Recent developments in deep learning have also sparked renewed interest for power system applications [6]–[9]. Deep feed-forward neural networks are used in [6] to predict the line currents for different N-1 outages. By encoding the system state inside the hidden layer of the neural network, the method can be applied to unseen N-2 outages with high accuracy [7]. The work in [8] proposes a deep autoencoder to reduce the high-dimensional input space of security assessment and increase classifier accuracy and robustness. Our work in [9] represents for the first time power system snapshots as images to take advantage of the advanced deep learning toolboxes for image processing, both currently available and in the future. Using convolutional neural networks, the method assesses both N-1 security and small signal stability at a fraction of the time required by conventional methods [9].

The neural network performance has been evaluated by splitting the available data in a training and a test set, and assess accuracy and other metrics on the previously unseen data of the test set (e.g. [6]–[9]). However, (i) this does not take into account that available data might not match the real-world distribution, (ii) it is not possible to anticipate how the network will classify new inputs, and (iii) only heuristic methods are available to identify adversarial examples.

Being able to determine the *range* of inputs that the neural network classifies as safe or unsafe renders the neural network interpretable. The previous statistical metrics such as accuracy are supported by provable guarantees of neural network behavior. This allows operators to either build trust in the neural network and use it in real-time operation, or decide to retrain it. At the same time, vulnerability to adversarial examples, i.e. small perturbations on the input leading to misclassifications, as shown in [10], pose a major threat to the use of neural networks in power systems. Increasing the robustness, and provably verifying target properties of these algorithms is therefore of high importance.

In this work, we present for the first time a framework to obtain formal guarantees of neural network behaviour for power system applications, using mixed-integer linear programming (MILP). In the rest of this paper, we refer to verification as the process of defining provable input regions in which the classification of the neural network does not change [11]. Our main contributions are:

- 1) This is the first work providing a framework to obtain formal guarantees for neural network behaviour in power system applications. This allows us to both provably verify target properties of neural networks (e.g. range

A. Venzke and S. Chatzivasileiadis are with the Department of Electrical Engineering, Technical University of Denmark, 2800 Kgs. Lyngby, Denmark e-mail: {andven, spchatz}@elektro.dtu.dk.

This work is supported by the multiDC project, funded by Innovation Fund Denmark, Grant Agreement No. 6154-00020.

of inputs classified as safe or unsafe) and to provably identify adversarial examples.

- 2) Formulating the verification problem as a mixed-integer linear program, we propose and test techniques to maintain scalability; these involve bound tightening and weight sparsification.
- 3) We demonstrate our methods on the IEEE 9-bus, 14-bus, and 162-bus system, treating both N-1 security and small-signal stability.

This work is structured as follows: In Section II, we describe the neural network architecture, in Section III we formulate the verification problem as a mixed-integer program and in Section IV we address tractability. In Section V we define our simulation setup and present results on formal guarantees for a range of power system security classifiers.

II. NEURAL NETWORK ARCHITECTURE AND TRAINING

A. Neural Network Structure

Before moving on with the formulation of the verification problem, in this section we explain the general structure of the neural networks we consider in this work [12]. An illustrative example is shown in Fig. 1. A neural network is defined by the number K of its fully-connected hidden layers, with each layer having N_k number of neurons (also called nodes or hidden units), with $k = 1, \dots, K$. The input vector is denoted with $\mathbf{x} \in \mathbb{R}^{N_0}$, and the output vector with $\mathbf{y} \in \mathbb{R}^{N_{K+1}}$. The input to each layer $\hat{\mathbf{z}}_{k+1}$ is a linear combination of the output of the previous layer, i.e. $\hat{\mathbf{z}}_{k+1} = \mathbf{W}_k \mathbf{z}_k + \mathbf{b}_k$, where \mathbf{W}_k is a $N_{k+1} \times N_k$ weight matrix and \mathbf{b}_k is a $N_{k+1} \times 1$ bias vector between layers k and $k+1$. Each neuron in the hidden layers incorporates an activation function, $z = f(\hat{z})$, which usually applies a non-linear transformation to the scalar input. There is a range of possible activation functions, such as the sigmoid function, the hyperbolic tangent, the Rectifier Linear Unit (ReLU), and others. Recent advances in computational power and machine learning have made possible the successful training of deep neural networks [13]. The vast majority of such networks use ReLU as the activation function as this has been shown to simplify their training. For the rest of this paper we will focus on ReLU as the chosen activation function. ReLU is a piecewise linear function defined as $z = \max(\hat{z}, 0)$. For each of the hidden layers we have:

$$\mathbf{z}_k = \max(\hat{\mathbf{z}}_k, 0) \quad \forall k = 1, \dots, K \quad (1)$$

$$\hat{\mathbf{z}}_{k+1} = \mathbf{W}_{k+1} \mathbf{z}_k + \mathbf{b}_{k+1} \quad \forall k = 0, 1, \dots, K-1 \quad (2)$$

where $\mathbf{z}_0 = \mathbf{x}$, i.e. the input vector. Throughout this work, the max operator on a vector $\hat{\mathbf{z}}_k \in \mathbb{R}^{N_k}$ is defined element-wise as $z_k^n = \max(\hat{z}_k^n, 0)$ with $n = 1, \dots, N_k$. The output vector is then obtained as follows:

$$\mathbf{y} = \mathbf{W}_{K+1} \mathbf{z}_K + \mathbf{b}_{K+1} \quad (3)$$

In this work, we will focus on classification networks, that is each of the output states y_i corresponds to a different class. For example, within the power systems context, each operating point \mathbf{x} can be classified as $y_1 = \text{safe}$ or $y_2 = \text{unsafe}$ (binary classification). Each input is classified to the category that corresponds to the largest element of the output vector \mathbf{y} . For example, if $y_1 > y_2$ then input \mathbf{x} is safe, otherwise unsafe.

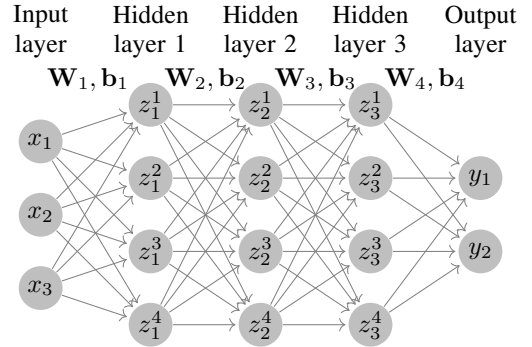


Fig. 1. Illustrative neural network for binary classification: Fully connected neural network with three inputs \mathbf{x} and three hidden layers. Between each layer, a weight matrix \mathbf{W} and bias \mathbf{b} is applied. Each hidden layer has four neurons with non-linear ReLU activation functions. Based on the comparison of the two outputs \mathbf{y} , the input is classified in one of the two categories, i.e. $y_1 > y_2$ or $y_1 < y_2$.

B. Neural Network Training

The training of neural networks requires a dataset of labeled samples \mathbf{S} , where each sample consists of the input \mathbf{x} and the output classification \mathbf{y} . The dataset is split into a training and a testing dataset. During training, the weights \mathbf{W} and biases \mathbf{b} are optimized for the training dataset with respect to a defined objective function. Different objective functions (also called loss functions) exist [12]. In this work we use one of the most commonly employed for classification: the softmax cross entropy, which is defined as follows. First, the softmax function takes the vector of the neural network output \mathbf{y} and transforms it to an equal-size vector of real numbers in the range between 0 and 1, the sum of which have to be equal to 1. This results to a probability p_i of the input belonging to the different classes $i \in N_{K+1}$:

$$p_i = \frac{e^{y_i}}{\sum_{j=1}^{N_{K+1}} e^{y_j}}, \quad \forall i \in N_{K+1} \quad (4)$$

Then, we can define the softmax cross entropy function:

$$\min_{\mathbf{W}, \mathbf{b}} f := - \sum_{i=1}^{N_{K+1}} y_i \log(p_i) \quad (5)$$

After training, we evaluate the neural network performance by calculating its accuracy on the unseen test dataset.

III. VERIFICATION AS A MIXED-INTEGER PROGRAM

As the accuracy on the test dataset is not sufficient to provide provable guarantees of neural network behavior, in the following, we formulate verification problems that allow us to verify target properties of neural networks and identify adversarial examples in a rigorous manner. Forming the verification problems as mixed-integer programs (MIP) enables us to develop a tractable computation method.

A. Reformulation of ReLU as Mixed Integer Program (MIP)

First, we reformulate the ReLU function $\mathbf{z}_k = \max(\hat{\mathbf{z}}_k, 0)$, shown in (1), using binary variables $\mathbf{r}_k \in \{0, 1\}^{N_k}$ [11]. For all $k = 1, \dots, K$, it holds:

$$\mathbf{z}_k = \max(\hat{\mathbf{z}}_k, 0) \Rightarrow \begin{cases} \mathbf{z}_k \leq \hat{\mathbf{z}}_k - \hat{\mathbf{z}}_k^{\min} (1 - \mathbf{r}_k) & (6a) \\ \mathbf{z}_k \geq \hat{\mathbf{z}}_k & (6b) \\ \mathbf{z}_k \leq \hat{\mathbf{z}}_k^{\max} \mathbf{r}_k & (6c) \\ \mathbf{z}_k \geq 0 & (6d) \\ \mathbf{r}_k \in \{0, 1\}^{N_k} & (6e) \end{cases}$$

The entries of the binary vector \mathbf{r}_k signal whether the corresponding ReLU unit in layer k is active or not. For a ReLU unit n , if $r_k^n = 0$, the ReLU is inactive and z_k^n is constrained to be zero through (6c) and (6d). Conversely, if r_k^n is 1, then z_k^n is constrained to be equal to \hat{z}_k^n through (6a) and (6b). The bounds on the ReLU output \hat{z}^{\min} and \hat{z}^{\max} have to be chosen sufficiently large to not be binding, but as low as possible to provide tight bounds in the branch-and-bound tree during the solution of the MIP. In Section IV-1, we present a possible approach to tighten these bounds using interval arithmetic (IA).

B. Formulating Verification Problems

Using (6a)-(6e), we can now verify neural network properties by formulating mixed integer linear programs. Without loss of generality, in this paper we assume that the neural network classifies the output in only two categories: y_1 and y_2 (e.g. safe and unsafe).

a) Verifying against adversarial examples: Assume a given input \mathbf{x}_{ref} is classified as y_1 , i.e. for the neural network output holds $y_1 > y_2$. Adversarial examples are instances close to the original input \mathbf{x}_{ref} that result to a different (wrong) classification [14]. Imagine for example an image of 2000×1000 pixels showing a green traffic light. An adversarial example exists if by changing just 1 pixel at one corner of the image, the neural network would classify it as a red light instead of the initial classification as green (e.g. see Fig. 16 of [15]). Machine learning literature reports on a wide range of such examples and methods for identifying them, as they can be detrimental for safety-critical application (such as autonomous vehicles). Due to the nature of this problem, however, most of these methods rely on heuristics. Verification can be a very helpful tool towards this objective as it can help us discard areas around given inputs by providing guarantees that no adversarial example exists.

Turning back to our problem, assume that the system operator knows that within distance ϵ from the operating point \mathbf{x}_{ref} the system remains safe ($y_1 > y_2$). If we can guarantee that the neural network will output indeed a safe classification for any input $\|\mathbf{x} - \mathbf{x}_{\text{ref}}\| \leq \epsilon$, then we can provide the operator with the guarantees required in order to deploy methods based on neural networks for real-time power system applications. To this end, we can solve the following mixed-integer program:

$$\min_{\mathbf{x}, \hat{\mathbf{z}}, \mathbf{z}, \mathbf{y}} y_1 - y_2 \quad (7a)$$

$$\text{s.t.} \quad (2), (3), (6a) - (6e) \quad (7b)$$

$$\|\mathbf{x} - \mathbf{x}_{\text{ref}}\|_* \leq \epsilon \quad (7c)$$

If the resulting objective function value is strictly positive (and assuming zero optimality gap), then $y_1 > y_2$ for all $\|\mathbf{x} - \mathbf{x}_{\text{ref}}\|_* \leq \epsilon$, and we can guarantee that no adversarial input exists within distance ϵ from the given point. The norm in (7c) can be chosen to be e.g. ∞ -norm, 1-norm or 2-norm. Here we focus on the ∞ -norm, which allows us to formulate the optimization problem (7) as mixed-integer linear program (MILP). Conversely, in case input \mathbf{x}_{ref} was originally classified as y_2 , we minimize $y_2 - y_1$ in objective function (7a) instead.

b) Adversarial robustness: Instead of solving (7) for a single ϵ , we can solve a series of optimization problems for different values of ϵ and assess the adversarial accuracy. The

adversarial accuracy is defined as the share of test samples \mathbf{s} that do not change classification within distance ϵ from the given input \mathbf{x}_{ref} . This can be used as an indicator for the robustness/brittleness of the neural network: low adversarial accuracy for very small ϵ is in most cases an indicator of poor neural network performance [16].

c) Computing largest regions with same classification:

To establish trust of neural networks among power system operators it is crucial to be able to determine the range of inputs a neural network will classify as safe or unsafe. The formulation (8) does that by computing the maximum input range around a given input \mathbf{x}_{ref} for which the classification will not change¹:

$$\min_{\mathbf{x}, \hat{\mathbf{z}}, \mathbf{z}, \mathbf{y}, \epsilon} \epsilon \quad (8a)$$

$$\text{s.t.} \quad (2), (3), (6a) - (6e) \quad (8b)$$

$$\|\mathbf{x} - \mathbf{x}_{\text{ref}}\|_* \leq \epsilon \quad (8c)$$

$$y_2 \geq y_1 \quad (8d)$$

Here again we select the ∞ -norm in (8c), turning (8) to a MILP. If input \mathbf{x}_{ref} is classified as y_2 , then we replace (8d) with $y_1 \geq y_2$ instead. Solving verification problem (8) enables us to provide the operator with guarantees that e.g. all system states where Generator 1 produces between 50 MW and 100 MW and Generator 2 produces between 30 MW and 80 MW, will be classified by the neural network as safe. Thus, the neural network is no longer a black box, and it is up to the operator to determine if its results are accurate enough. If they are not, the operator can retrain the neural network with adjusted parameters to increase the accuracy for regions the operator is mostly interested. Alternatively, the operator can follow a risk-based approach attaching a certain confidence/risk level to the neural network results, or the operator can choose to use the neural network for a limited range of inputs where its results are provably 100% accurate.

d) Input constraints: In all verification problems, we can add additional constraints characterizing the admissible region for the input vector \mathbf{x} and, thus, can obtain larger regions with the same classification. Given that in neural network training it is standard practice to normalize the input between 0 and 1, we add constraint (9) to both formulations in (7) and (8):

$$\mathbf{0} \leq \mathbf{x} \leq \mathbf{1} \quad (9)$$

In Section V-B, we will show how including the DC power balance (11) as additional constraint on the input allows to further improve the obtained bounds in (8a).

IV. IMPROVING TRACTABILITY OF VERIFICATION PROBLEMS

By examining the complexity of the MILPs presented in Section 3, we make two observations. First, from (6a) - (6e) it becomes apparent that the number of required binaries in the MILP is equal to the number of ReLU units in the neural network. Second, the weight matrices \mathbf{W} are dense as the neural network layers are fully connected. As neural networks can potentially have several hidden layers with a large number of hidden neurons, improving the computational tractability of

¹Note that we achieve this by computing the *minimum* distance to a sample which *does* change the classification.

the MILP problems is necessary. To this end, we apply two different methods: tightening the bounds on the ReLU output, and sparsifying the weight matrices.

1) *ReLU bound tightening*: In the reformulation of the maximum operator in (6a) and (6c), we introduced upper and lower bounds $\hat{\mathbf{z}}^{\max}$ and $\hat{\mathbf{z}}^{\min}$, respectively. Without any specific knowledge about the bounds, these have to be set to a large value in order not to become binding. A computationally cheap approach to tighten the ReLU bounds is through interval arithmetic (IA) [11]. We propagate the initial bounds on the input $\mathbf{z}_0^{\min} = \mathbf{x}^{\min}$, $\mathbf{z}_0^{\max} = \mathbf{x}^{\max}$ through each layer to obtain individual bounds on each ReLU in layer $k = 1, \dots, K$:

$$\hat{\mathbf{z}}_k^{\max} = \hat{\mathbf{z}}_{k-1}^{\max,+} \mathbf{W}_{k-1}^+ + \hat{\mathbf{z}}_{k-1}^{\min,+} \mathbf{W}_{k-1}^- + \mathbf{b}_{k-1} \quad (10a)$$

$$\hat{\mathbf{z}}_k^{\min} = \hat{\mathbf{z}}_{k-1}^{\min,+} \mathbf{W}_{k-1}^+ + \hat{\mathbf{z}}_{k-1}^{\max,+} \mathbf{W}_{k-1}^- + \mathbf{b}_{k-1} \quad (10b)$$

The max and min-operator are denoted in compact form as: $\mathbf{x}^+ = \max(\mathbf{x}, 0)$ and $\mathbf{x}^- = \min(\mathbf{x}, 0)$. Methods to compute tighter bounds also exist, e.g. by solving an LP relaxation while minimizing or maximizing the ReLU bounds [17], but this is out of scope of this paper.

2) *Training Neural Networks for Easier Verifiability*:

A second possible approach to increase the computational tractability of the verification problems is to re-train the neural network with the additional goal to sparsify the weight matrices \mathbf{W} . Here, we rely on an automated gradual pruning algorithm proposed in [18]. Starting from 0% sparsity, where all weight matrices \mathbf{W} are non-zero, a defined share of the weight entries are set to zero. The weight entries selected are those with the smallest absolute magnitude. Subsequently, the neural network is re-trained for the updated sparsified structure. This procedure is repeated until a certain sparsity target is achieved. There are two important observations: First, through sparsification the classification accuracy can decrease, as less degrees of freedom are available during training. Second, larger sparsified networks can achieve better performance than smaller dense networks [18]. As a result, by forming slightly larger neural networks we can maintain the required accuracy while achieving sparsity. As we will see in Section V, sparsification maintains a high classification accuracy and, thus, a significant computational speed-up is achieved when solving the MILPs. As a further benefit of sparsification, the interpretability of the neural network increases, as the only neuron connections kept are the ones that have the strongest contribution to the classification. Computational tractability can further increase by pruning ReLUs during training, i.e. fixing them to be either active or inactive, in order to eliminate the corresponding binaries in the MILP [19]. This approach along with the LP relaxation for bound tightening will be object of our future work.

V. SIMULATION AND RESULTS

A. *Simulation Setup*

Our methodology consists of three main steps: (i) creating a dataset to train and test our neural network, (ii) training the neural network, and (iii) converting the neural network to a MILP in order to verify its behavior. The rest of this subsection details the procedure.

The created dataset can include both historical and simulated operating points. Absent historical data in this paper, we

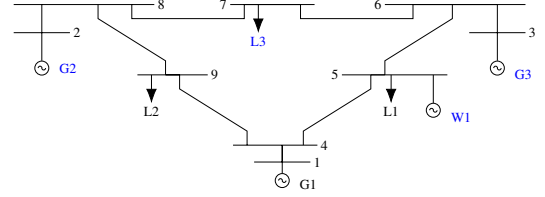


Fig. 2. Modified IEEE 9-bus system with wind farm $W1$ at bus 5, and uncertain load at bus 7. Generation and loading marked in blue correspond to the input vector \mathbf{x} of the neural network.

created simulated data for our studies. Using Latin Hypercube Sampling (LHS), we draw a defined number of samples $|\mathbf{S}|$ in the input space $\mathbf{x} \in \mathbf{X}$ of the neural network. LHS allows to maximize the distance between the individual samples and cover the possible input space evenly. To facilitate a more efficient neural network training procedure, we subsequently normalize each entry of the input vector \mathbf{x} to be between 0 and 1 using the upper and lower bounds of the variables (we do that for all samples $\mathbf{x} \in \mathbf{S}$).

Training dataset \mathbf{S} shall include both inputs \mathbf{x} and expected outputs \mathbf{y} . Therefore, for each chosen sample, we shall compute the classification output ‘safe’ or ‘unsafe’ based on the selected security criteria. In this paper, we use two types of security criteria. For the IEEE 9-bus system, in order to help the reader gain the required insights, we employ the N-1 security criterion based on the DC power flow, and use the MATPOWER to determine the safe/unsafe classification for each sample [20]. We do the same for the 162-bus system, where we demonstrate the scalability of our methods. Finally, for the IEEE 14-bus system, we employ the *combination* of N-1 security based on AC power flow *and* small-signal stability as a security criterion. The method for creating such a dataset is detailed in our work [21].

After creating the training dataset, we export it to TensorFlow [22] for the neural network training. We split the dataset into a training set and a test set. We choose to use 85% of samples for training and 15% for testing. During training, we minimize the cross-entropy loss function (5) using the Adam optimizer with stochastic gradient descent [22], and use the default options in TensorFlow for training. In the cases where we need to enforce a certain sparsity of the weight matrices we re-train with the same objective function (5), but during training we reduce the number of non-zero weights until a certain level of sparsity is achieved, as explained in Section IV-2.

To allow for the neural network verification and the identification of adversarial examples, after the neural network training we export the weight matrices \mathbf{W} and biases \mathbf{b} in YALMIP, formulate the MILPs, and solve them with Gurobi. If not noted otherwise, we solve all MILPs to zero optimality gap, and as a result obtain the globally optimal solution. All simulations are carried out on a laptop with processor Intel(R) Core(TM) i7-7820HQ CPU @ 2.90 GHz and 32GB RAM.

B. *Neural Network Verification for the IEEE 9-bus system*

1) *Test Case Setup*: We consider a modified IEEE 9-bus system shown in Fig. 2. This system has three generators and one wind farm. We assume that the load at bus 7 is uncertain and can vary between 0 MW and 200 MW. The wind farm output is uncertain as well and can vary between 0 MW and 300 MW. The line limits are increased by 25%

TABLE I
CONFUSION MATRICES FOR IEEE 9-BUS TEST CASE

Neural network <u>without</u> sparsity			
Test samples: 1500	Predicted: Safe	Unsafe	Accuracy
True: Safe (326)	311	15	98.3%
True: Unsafe (1174)	11	1163	
Neural network <u>with</u> 80% sparsity			
Test samples: 1500	Predicted: Safe	Unsafe	Accuracy
True: Safe (326)	308	18	97.8%
True: Unsafe (1174)	15	1159	

to accommodate the added wind generation and increased loading. Remaining parameters are defined according to [20]. As mentioned in the previous subsection, in this case we employ the N-1 security for the DC power flow as a security criterion. To compute the ground truth (and thus be able to assess the neural network performance) we use the N-1 preventive security constrained DC-OPF (SC-DC-OPF) fixing each time all relevant constraints equal to the specified input, as this allows us to consider all critical outages in a single algorithm. If the SC-DC-OPF results to infeasibility, then the sample is ‘unsafe’. We consider the single outage of each of the six transmission lines and use MATPOWER. We create a dataset of 10’000 possible operating points with input vector $\mathbf{x} = [P_{G2} P_{G3} P_{L3} P_{W1}]$, which are classified $\mathbf{y} = \{y_1 = \text{safe}, y_2 = \text{unsafe}\}$. Note that the first generator P_{G1} is the slack bus and its power output is uniquely determined through the dispatch of the other units; therefore, it is not considered as input to the neural network.

2) *Neural Network Training*: Using the created dataset, we train two neural networks which only differ with respect to the enforced sparsity of the weight matrices. Employing loss function (5), the first neural network is trained with dense \mathbf{W} matrices. Using this as a starting point for the retraining, on the second neural network we enforce 80% sparsity, i.e. only 20% of the $\mathbf{W}^{\text{sparse}}$ entries are allowed to be non-zero. In both cases, the neural network architecture comprises three hidden layers with 50 neurons each, as this allows us to achieve high accuracy without over-fitting. For comparison, if we would only train a single-layer neural network with 150 neurons, the maximum test set classification accuracy is only 90.7%, highlighting the need for a multi-layer architecture.

Our three-layer neural network without sparsity has a classification accuracy of 98.3% on the test set and 98.4% on the training set. This illustrates that neural networks can predict with high accuracy whether an operating point is safe or unsafe. If we allow only 20% of the \mathbf{W} entries to be non-zero and re-train the three-layer neural network, the classification accuracy evaluates to 97.8% on the test set and 97.3% on the training set. The corresponding confusion matrices for both neural networks for the test set are shown in Table I. As we see, the sparsification of the neural network leads to a small reduction of 0.5% in classification accuracy, since less degrees of freedom are available during training. The benefits from sparsification are, however, substantially more significant. As we will see later in our analysis, sparsification substantially

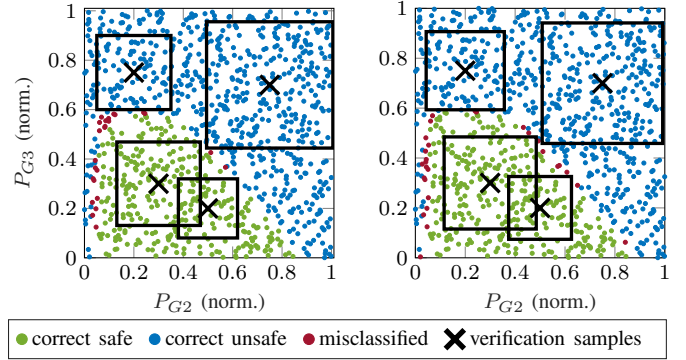


Fig. 3. Regions around four verification samples in which the classification is guaranteed not to change. The left figure uses the neural network without sparse weight matrices, and the right figure uses the neural network with imposed 80% sparsity on the weight matrices. For visualization purposes, the load P_{L3} and wind level P_{W1} are fixed to 40% and 1’000 new samples are created and classified according to the respective neural network.

increases the computational tractability of verification problems, and leads to an increase in interpretability of the neural network. Both are necessary to remove barriers for adopting neural networks in safety-critical systems.

3) *Visualization of Verification Samples*: To be able to visualize the input regions for which we can guarantee that the trained neural networks will not change their classification, we shall reduce the input dimensionality. For this reason, we will study here only a single uncertainty realization, where we assume that both the load P_{L3} and wind power output P_{W1} amount to 40% of their normalized output (note that our results apply to all possible inputs). The resulting input space is two-dimensional and includes generators P_{G2} and P_{G3} . For visualization purposes only, we take 1’000 new samples from the reduced two-dimensional space and classify them with the neural networks as safe or unsafe. In addition, we compute their true classification using MATPOWER. The resulting classified input spaces are shown in Fig. 3 with the left figure corresponding to the neural network with full weight matrices \mathbf{W} , and the right figure to the sparsified weight matrices $\mathbf{W}^{\text{sparse}}$. We can observe that misclassifications occur at the security boundary. This is to be expected as the sampling for this visualization is significantly more dense than the one used for training. What is important here to observe though, is that even if the neural network on the right contains only 20% of the original number of non-zero weights, the neural networks have visually comparable performance in terms of classification accuracy.

As a next step, we solve the verification problem described in (8). In that, for several samples \mathbf{x}_{ref} we compute the minimum perturbation ϵ that changes the classification. We visualize the obtained regions using black boxes around the verification samples in Fig. 3. The average solving time in Gurobi is 5.5 s for the non-sparsified and 0.3 s for the sparsified neural network. We see that by sparsifying the weights we achieve a 20 \times computational speed-up. Solving the MILP to zero optimality gap, we are guaranteed that within the region defined by the black boxes around the verification samples no input $\mathbf{x} \in [0, 1]$ exists which can change the classification. As will be shown in Section V-D3, as a following step we could also evaluate the verification problems (7) for different values

TABLE II
VERIFICATION OF NEURAL NETWORK PROPERTIES FOR 9-BUS SYSTEM

	w/o power balance		with power balance	
	ϵ	Sol. Time (s)	ϵ	Sol. Time (s)
Property 1: $\forall x \in [0, 1] : x - \mathbf{1} _\infty \leq \epsilon \rightarrow$ Classification: insecure				
NN (w/o sparsity)	50.7%	2.7 IA: 1.1	54.4%	1.5 IA: 1.3
NN (80% sparsity)	48.7%	0.3 IA: 0.2	54.4%	0.3 IA: 0.2
SC-DC-OPF	53.7%	-	53.7%	-
Property 2: $\forall x \in [0, 1] : x - \mathbf{0} _\infty \leq \epsilon \rightarrow$ Classification: secure				
NN (w/o sparsity)	29.2%	501.9 IA: 400.7	29.3%	473.0 IA: 817.9
NN (80% sparsity)	32.7%	3.3 IA: 1.1	32.7%	2.1 IA: 1.6
SC-DC-OPF ²	31.7%	-	31.7%	-
Property 3: $\exists x \in [0, 1] : P_{W2} - \mathbf{0} _\infty \leq \epsilon \rightarrow$ Classification: secure				
NN (w/o sparsity)	97.4%	12.2 IA: 11.4	90.3%	6.5 IA: 3.7
NN (80% sparsity)	99.1%	0.4 IA: 0.3	89.0%	0.4 IA: 0.3
SC-DC-OPF	92.5%	-	92.5%	-

² The SC-DC-OPF can only provide infeasibility certificates.

We compute this by re-sampling a very large number of samples.

of ϵ for every test and training sample to obtain the adversarial accuracy of a neural network.

4) *Provable Guarantees:* In the following, we want to provide several provable guarantees of behaviour for both neural networks while considering the entire input space. For this purpose, we solve verification problems of the form (8). Since the neural network input \mathbf{x} is normalized between $\mathbf{0} \leq \mathbf{x} \leq \mathbf{1}$ based on the bounds of the input variables $\mathbf{x}^{\min}, \mathbf{x}^{\max}$, we include the corresponding constraint (9) in the verification problem. Similarly, no input to the neural network would violate P_{G1} limits. Even if P_{G1} is not part of the input, its limits can be propagated to input \mathbf{x} through the DC power balance, as shown in (11):

$$P_{G1}^{\min} \leq \sum_{i=1}^{N_1} x_i (x_i^{\max} - x_i^{\min}) + x_i^{\min} \leq P_{G1}^{\max}, \quad (11)$$

where $\mathbf{x} = [x_i]^T = [P_{G2} P_{G3} P_{L3} P_{W1}]^T$. In this section, we show how additional a-priori qualifications of the input such as (11), affect the size of the regions in which we can guarantee a certain classification.

In Table II, we compare the obtained bounds to the ground truth provided by the SC-DCOPF and report the computational time for three properties, when we do not include and when we do include the power balance constraint. The second reported computational time uses the tightened ReLU bounds (10) with interval arithmetic (IA) (see Section IV-1 for details on the method). The first property is the size of the region around the $\mathbf{x}_{\text{ref}} = \mathbf{1}$ (1-vector), which corresponds to the maximum generation and loading of the system. For this input, the classification of the neural networks is known to be unsafe. We observe for both neural networks that when the power balance constraint is not included in the verification problem, the input region guaranteed to be classified as unsafe is smaller than the ground truth of 53.7% (provided by the SC-DC-OPF). By including the power balance in the verification problem, the input region classified as unsafe is significantly enlarged and more closely matches the target of 53.7%.

For the second property, we consider the region around the operating point where all generating units and the load are at their lower bound \mathbf{x}^{\min} , that is $\mathbf{x}_{\text{ref}} = \mathbf{0}$. This point corresponds

to a low loading of the system and is therefore secure (i.e. no line overloadings, etc.). We solve the verification problem minimizing the distance from $\mathbf{x}_{\text{ref}} = \mathbf{0}$ leading to an insecure classification. In this way, we obtain the maximum region described as hyper-cube around the zero vector in which the classification is guaranteed to be always ‘safe’. We can observe in this case that the neural network without sparsity slightly underestimates while the neural network with 80% sparsity slightly overestimates the safe region compared to the ground truth (31.7%). Sparsification allows a $150 \times - 500 \times$ computational speed-up (two orders of magnitude). For this property, including the power balance constraint does not change the obtained bounds.

The third property we analyze is the maximum wind infeed for which the neural network identifies a secure dispatch. To this end, we solve the verification problem by maximizing the wind infeed P_{W1} in the objective function while maintaining a secure classification. The true maximum wind infeed obtained by solving this problem directly with the SC-DC-OPF is 92.5%, i.e. 277.5 MW can be accommodated. If we do not enforce constraint (11), then we observe that the obtained bounds 97.4% and 99.12% are not tight. This happens because the obtained solutions \mathbf{x} from (8) keep generation and loading to zero and only maximize wind power; this violates the generator bounds on the slack bus, as it has to absorb all the generated wind power. By enforcing the DC power balance (11) in the verification problem, allows a more accurate representation of the true admissible inputs, and we obtain significantly improved bounds of 90.3% and 89.0%.

For all three properties, we observe that both interval arithmetic (IA) and weight sparsification improve computational tractability, in most instances achieving the lowest solver times when used combined. From the two, weight sparsification has the most substantial effect as it allows to reduce the number of binaries in the resulting MILP problem.

C. Scalability for IEEE 162-bus system

1) *Test Case Setup:* We consider the IEEE 162-bus system with parameters taken from [20]. We add five uncertain wind generators located at buses $\{3, 20, 25, 80, 95\}$ with a rated power of 500 MW each. As security criterion, we consider again N-1 security based on DC power flow, considering the outage of 24 critical lines: $\{22, \dots, 27, 144, \dots, 151, 272, \dots, 279\}$. The input vector is defined as $\mathbf{x} = [P_{G1-G12} P_{W1-W5}]^T$. To construct the dataset for the neural network training, we first apply a bound tightening of the generator active power bounds, i.e. we maximize and minimize the corresponding bound considering the N-1 SC-DC-OPF constraints. The tightened bounds exclude regions in which the SC-DC-OPF is guaranteed to be infeasible and therefore allows to decrease the input space. In the remaining input space, we draw 10^6 samples using latin hypercube sampling (LHS) and classify them as safe or unsafe. As usual in power system problems, the ‘safe’ class is substantially smaller than the ‘unsafe’ class, since the true safe region is only a small subset of the eligible input space. To mitigate the dataset imbalance, we compute the closest feasible dispatch for each of the infeasible samples by solving an SC-DC-OPF problem and using the ∞ -norm as distance metric. As a result, we obtain a balanced dataset of approximately 20^6 samples.

TABLE III
CONFUSION MATRIX FOR IEEE 162-BUS TEST CASE (WITH SPARSITY)

Test samples: 3000	Predicted: Safe	Unsafe	Accuracy
True: Safe (1507)	1501	6	
True: Unsafe (1493)	11	1482	
Accuracy			99.4%

TABLE IV
VERIFICATION OF NEURAL NETWORK PROPERTIES FOR 162-BUS SYSTEM

	w/o power balance		with power balance	
	ϵ	Sol. Time (s)	ϵ	Sol. Time (s)
Property 1: $\forall x \in [0, 1] : x - 0 _\infty \leq \epsilon \rightarrow$ Classification: insecure				
NN (w/o sparsity)	-	> 50 min	-	> 50 min
NN (80% sparsity)	59.4%	560 IA: 1217	65.5%	22 IA: 30
SC-DC-OPF	66.2%	-	66.2%	-

2) *Neural Network Training*: We choose a neural network architecture with 4 layers of 100 ReLU units at each layer, as the input dimension increases from 4 to 17 compared to the 9-bus system. We train again two neural networks: one without enforcing sparsity and a second with 80% sparsity. The trained four-layer network without sparsity has a classification accuracy 99.3% on the test set and 99.7% on the training set. For the sparsified network, these metrics evaluate to 99.7% for the test set and 99.4% for the training set. The confusion matrix of the sparsified network is shown in Table III and it can be observed that the neural network has high accuracy in classifying both safe and unsafe operating points.

3) *Provable Guarantees*: Assuming the given load profile, the property of interest is to determine the minimum distance from zero generation $\mathbf{x}_{\text{ref}} = \mathbf{0}$ to a feasible ('safe') solution. In Table IV, we compare the result of the verification problem with the ground truth obtained from solving the SC-DC-OPF problem. We can see that the bound of 59.4% we obtain without including the DC power balance is not tight compared to the ground truth of 66.2%. Including the DC power balance increases the bound to 65.2% which is reasonably close, indicating satisfactory performance with respect to this property. This confirms the findings for the 9-bus (cmp. Tables II and IV) showing that including the additional power balance constraint in the verification problems leads to bounds on ϵ closer to the ground-truth. Regarding computational time, we can observe that for this larger neural network, the sparsification of the weight matrices becomes a requirement to achieve tractability. For both cases with and without including the DC power balance, the MILP solver did not identify a solution after 50 minutes for the non-sparsified network.

D. N-1 Security and Small Signal Stability

Security classifiers using neural networks can screen operating points for security assessment several orders of magnitudes faster than conventional methods [9]. There is, however, a need to obtain guarantees for the behaviour of these classifiers. We show in the following how our framework allows us to analyse the performance of a classifier for both N-1 security and small signal stability.

1) *Test Case Setup*: Here, we consider the IEEE 14-bus system [20] and create a dataset of operating points which are classified according to their feasibility to *both* the N-1

TABLE V
CONFUSION MATRIX FOR IEEE 14-BUS TEST CASE (WITH SPARSITY)

Test samples: 1500	Predicted: Safe	Unsafe	Accuracy
True (15): Safe	12	3	
True (1485): Unsafe	0	1485	
Accuracy			99.8%

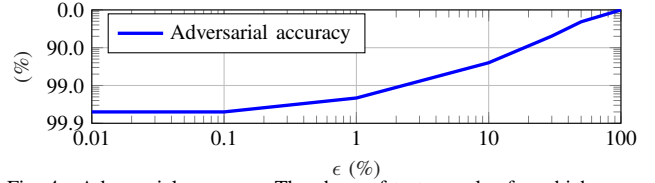


Fig. 4. Adversarial accuracy: The share of test samples for which a sample exist within distance ϵ which changes the classification. Note that both axes are logarithmic and the y-axis runs from 100% to 0%.

SC-AC-OPF problem and small signal stability. For a detailed overview of the modeling assumptions please refer to [21] and references therein. We use a simple brute-force sampling strategy to create a dataset of 10'000 equally spaced points in the four input dimensions $\mathbf{x} = [P_{G2-G5}]$. Note that, similar to the 162-bus case, the dataset is unbalanced as only 1.36% of the overall created samples are feasible. A method to create balanced datasets for *both* static and dynamic security is object of future work.

2) *Neural Network Training*: We choose a three-layer neural network with 50 neurons for each layer, as in Section V-B. Based on the analysis of the previous case studies, here we only train an 80% sparsified network. The network achieves the same accuracy of 99.8% both on the training and on the test set. The confusion matrix on the test set is shown in Table V. Note that here the accuracy does not carry sufficient information as a metric of the neural network performance, as simply classifying all samples as unsafe would lead to a test set accuracy of 99.0% due to the unbalanced classes. Besides the use of supplementary metrics, such as specificity and recall (see e.g. [9]), obtaining provable guarantees of the neural network behavior becomes, therefore, of high importance. In the following, to obtain such guarantees we assess the adversarial accuracy of the neural network and identify an adversarial example.

3) *Evaluating Adversarial Accuracy*: Adversarial accuracy identifies the number of samples whose classification changes if we perform a perturbation to their input. Assuming that points in the neighborhood of a given sample should share the same classification, e.g. points around a 'safe' sample would likely be safe, a possible classification change indicates that we are either very close to the security boundary or we might have discovered an adversarial example. Carrying out this procedure for our whole dataset, we would expect that in most cases the classification in the vicinity of the sample will not change (except for the comparably small number of samples that is close to the security boundary). In Fig. 4 the adversarial accuracy is depicted for the sparsified neural network. It can be observed that for small perturbations, i.e. $\epsilon \leq 1\%$, the adversarial accuracy stays well above 99%; that is, for 99% of test samples no input exists within distance of ϵ which changes the classification. Only if large perturbations to the input are allowed (i.e. $\epsilon \geq 1\%$) the adversarial accuracy

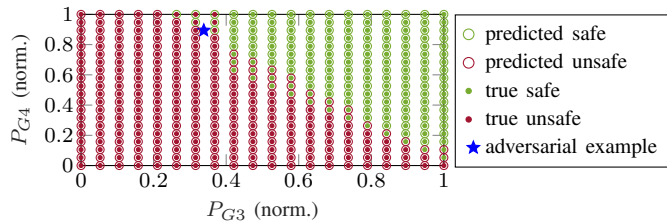


Fig. 5. Classification of 400 new equally spaced samples for the IEEE 14-bus system. For 2-D visualization purposes, the active power of P_{G2} and P_{G5} are fixed to their maximum output. Blue star marks an identified adversarial example. The reason is the inaccurate prediction of the system security boundary.

decreases. This shows that the classification of our neural network is adversarially robust in most instances. Note that the adversarial accuracy only makes a statement regarding the classification by the neural network and is not related to the ground truth classification. In a subsequent step, as we show in the next paragraph, we need to assess whether identified samples are in fact misclassified.

4) *Identifying Adversarial Examples:* Having identified regions where adversarial examples may exist, we can now proceed with determining if they truly exist. Focusing on the test samples which are not adversarially robust for small ϵ , i.e. $\epsilon \leq 1\%$, we identify an adversarial example for the sample $\mathbf{x} = [1.0, 1.0, 0.3333, 0.8889]$ with classification ‘unsafe’. Modifying this input only by $\epsilon = 0.5\%$, we identify the adversarial input $\mathbf{x}_{adv} = [1.0, 1.0, 0.3383, 0.8939]$ which falsely changes the classification to ‘safe’, i.e. $y_{adv,1} > y_{adv,2}$. In Fig. 5 the location of the adversarial example is marked by a star. For illustrative purposes in Fig. 5, we re-sample 400 equally spaced samples and compute both the neural network prediction and ground truth. We can observe that the neural network boundary prediction is not precise and as a result, the adversarial input gets falsely classified as safe. Note that in the confusion matrix of the test set (Table V) no unsafe sample has been falsely classified as safe, i.e. this property cannot be detected by solely analyzing the confusion matrix. This highlights the additional benefit of the presented framework to identify adversarial examples, and subsequently regions in which additional detailed sampling is necessary. Directions for improving the performance of the neural network include to (i) re-sample around adversarial examples, (ii) use a dataset creation method that provides a more detailed description of the security boundary e.g. using the algorithm in [21], and (iii) re-train the neural networks to be adversarially robust, i.e. modify the objective function (5) as outlined e.g. in [16].

VI. CONCLUSION

Neural networks in power system applications have so far been treated as a black box; this has become a major barrier towards their application in practice. This is the first work to present a rigorous framework for neural network verification in power systems and obtain provable performance guarantees. To this end, we formulate the verification problem as a mixed-integer linear program and train neural networks to be computationally easier verifiable. We provably determine the range of inputs that are classified as safe or unsafe, and identify adversarial examples, i.e. slight modifications in the input that lead to a mis-classification by neural networks. This enables power system operators to understand and anticipate the neural

network behavior, building trust in them, and remove a major barrier toward their adoption in power systems. We verify properties of a security classifier for an IEEE 9-bus system and demonstrate its scalability for a 162-bus system, highlighting the need for sparsification of neural network weights. Finally, we further identify adversarial examples and evaluate the adversarial accuracy of neural networks trained to assess both N-1 security and small-signal stability.

REFERENCES

- [1] P. Panciatici *et al.*, “Advanced optimization methods for power systems,” in *2014 Power Systems Computation Conference*. IEEE, 2014.
- [2] L. A. Wehenkel, *Automatic learning techniques in power systems*. Springer Science & Business Media, 2012.
- [3] L. Duchesne, E. Karangelos, and L. Wehenkel, “Using machine learning to enable probabilistic reliability assessment in operation planning,” in *2018 Power Systems Computation Conference*. IEEE, 2018.
- [4] G. Dalal, E. Gilboa, S. Mannor, and L. Wehenkel, “Chance-constrained outage scheduling using a machine learning proxy,” *IEEE Transactions on Power Systems*, 2019.
- [5] S. R. R. S. Kumar, and A. T. Mathew, “Online static security assessment module using artificial neural networks,” *IEEE Transactions on Power Systems*, vol. 28, no. 4, pp. 4328–4335, Nov 2013.
- [6] B. Donnot, I. Guyon, M. Schoenauer, P. Panciatici, and A. Marot, “Introducing machine learning for power system operation support,” *CoRR, arXiv preprint arXiv:1709.09527*, 2017.
- [7] B. Donnot, I. Guyon, M. Schoenauer, A. Marot, and P. Panciatici, “Fast power system security analysis with guided dropout,” *CoRR, arXiv preprint arXiv:1801.09870*, 2018.
- [8] M. Sun, I. Konstantelos, and G. Strbac, “A deep learning-based feature extraction framework for system security assessment,” *IEEE Transactions on Smart Grid*, 2018.
- [9] J.-M. H. Artega, F. Thams, and S. Chatzivasileiadis, “Deep learning for power system security assessment,” in *13th IEEE PowerTech 2019*. IEEE, 2019.
- [10] Y. Chen, Y. Tan, and D. Deka, “Is machine learning in power systems vulnerable?” in *2018 IEEE SmartGridComm*. IEEE, 2018, pp. 1–6.
- [11] V. Tjeng, K. Y. Xiao, and R. Tedrake, “Evaluating robustness of neural networks with mixed integer programming,” in *International Conference on Learning Representations (ICLR 2019)*, 2019. [Online]. Available: <https://openreview.net/forum?id=HyGIIdiRqtm>
- [12] C. Bishop, *Pattern Recognition and Machine Learning*. Springer, 2006.
- [13] Y. LeCun, Y. Bengio, and G. Hinton, “Deep learning,” *Nature*, vol. 521, pp. 436–444, 2015.
- [14] I. J. Goodfellow, J. Shlens, and C. Szegedy, “Explaining and harnessing adversarial examples,” *arXiv preprint arXiv:1412.6572*, 2014.
- [15] M. Wu *et al.*, “A game-based approximate verification of deep neural networks with provable guarantees,” *Theoretical Computer Science*, 2019.
- [16] A. Madry, A. Makelov, L. Schmidt, D. Tsipras, and A. Vladu, “Towards deep learning models resistant to adversarial attacks,” in *International Conference on Learning Representations (ICLR 2018)*, 2018. [Online]. Available: <https://openreview.net/forum?id=rJzIBfZAb>
- [17] K. Dvijotham, R. Stanforth, S. Gowal, T. Mann, and P. Kohli, “A dual approach to scalable verification of deep networks,” in *UAI-18*. Corvallis: AUAI Press, 2018, pp. 162–171.
- [18] M. Zhu and S. Gupta, “To prune, or not to prune: exploring the efficacy of pruning for model compression,” *arXiv preprint 1710.01878*, 2017.
- [19] K. Y. Xiao, V. Tjeng, N. M. M. Shafiqullah, and A. Madry, “Training for faster adversarial robustness verification via inducing ReLU stability,” in *International Conference on Learning Representations (ICLR 2019)*, 2019. [Online]. Available: <https://openreview.net/forum?id=BJfIVjAcKm>
- [20] R. D. Zimmerman, C. E. Murillo-Sánchez, and R. J. Thomas, “Matpower: Steady-state operations, planning, and analysis tools for power systems research and education,” *IEEE Transactions on Power Systems*, vol. 26, no. 1, pp. 12–19, 2010.
- [21] F. Thams, A. Venzke, R. Eriksson, and S. Chatzivasileiadis, “Efficient database generation for data-driven security assessment of power systems,” *IEEE Transactions on Power Systems*, 2019.
- [22] M. Abadi *et al.*, “TensorFlow: Large-scale machine learning on heterogeneous systems,” 2015, software available from tensorflow.org. [Online]. Available: <https://www.tensorflow.org/>